ARTICLES
PUBLISHED ONLINE: 21 AUGUST 2011 | DOI: 10.1038/NPHOTON.2011.177
nature photonics

Giant broadband nonlinear optical absorption response in dispersed graphene single sheets

Geok-Kieng Lim[1,2]*, Zhi-Li Chen[2], Jenny Clark[4], Roland G. S. Goh[3], Wee-Hao Ng[1], Hong-Wee Tan[1], Richard H. Friend[2,4], Peter K. H. Ho[2] and Lay-Lay Chua[2,3,4]*

Under intense laser excitation, thin films and suspensions of graphite and its nanostructure, including carbon black, nanotubes, few-layer graphenes and graphene oxides, exhibit induced transparency due to saturable absorption. This switches to optical limiting only at very high fluences when induced breakdown gives rise to microbubbles and microplasmas that causes nonlinear scattering. Here, we show that dispersed graphenes, in contrast, can exhibit broadband nonlinear optical absorption at fluences well below this damage threshold with a strong matrix effect. We obtained, for nanosecond visible and near-infrared pulses, a new benchmark for optical energy-limiting onset of 10 mJ cm^{-2} for a linear transmittance of 70%, with excellent output clamping in both heavy-atom solvents and polymer film matrices. Nanosecond pump–probe spectroscopy in chlorobenzene reveals that the nanographene domains switch from the usual broadband photo-induced bleaching to a novel reverse saturable absorption mechanism with increasing excitation densities across this threshold.

There is significant interest in manipulating the intensity and shape of laser pulses in a number of advanced optical technologies using nonlinear optical (NLO) materials[1]. There are two main classes of such materials: (i) saturable absorbers, which give increased transmittance at high optical intensities or fluences, and are useful for pulse compression, Q-switching and mode locking; and (ii) optical limiters, which give decreased transmittance, and are useful not only for pulse shaping and mode locking, but also for the protection of eyes and sensor focal-plane arrays.

Significant progress has been made over recent decades in the development of optical limiters with large NLO responses, particularly in carbon-based materials[2]. These include graphitic systems such as carbon black suspensions (CBS)[3,4], single-walled and multi-walled carbon nanotubes (CNTs)[5–7] and small π-electron systems such as fullerenes[8,9], porphyrins and phthalocyanines[10–12]. A large part of this effort has been directed towards developing materials that can be processed as stable solutions or liquid dispersions that can ultimately be formed into films for practical applications.

For over a decade now, the optical-limiting benchmark for broadband (wide spectrum) limiting has been held by CBS and CNT suspensions[3–7]. These limit the transmission of optical energy by nonlinear scattering when solvent microbubbles and/or microplasmas are formed at high fluences[3,4,13]. However, neither mechanism is effective against pulses shorter than a few nanoseconds because of the required breakdown time. They are also ineffective in solid films where there is no solvent and breakdown of the material leads instead to the formation of pinholes[3]. The small π-electron systems, on the other hand, can provide optical-limiting properties by means of excited-state absorption of long-lived triplet states formed in the sub-nanosecond timescale[2]. This mechanism can provide highly effective optical limitation in liquid cells and solid films, but only over narrow wavelength bands because of the strong wavelength dependence of the ratio of excited-state to ground-state absorption cross-sections. Recently, suspensions of graphene and graphene oxides (GOx) have also been shown to give broadband optical-limiting characteristics in a variety of solvents[14–16]. Their limiting thresholds and output clamping characteristics are, however, broadly similar to those of CBS and CNT suspensions, and the mechanism is also nonlinear scattering[14]. This suggests that a number of graphitic nanostructures share similar NLO behaviour.

We demonstrate here that when graphene is functionalized and dispersed as single sheets in heavy-atom solvents or in certain film matrices, it exhibits a novel excited-state absorption mechanism that can provide highly effective optical limitation across the visible and near-infrared spectral regions, at pulse fluences well below the onset of microbubble or microplasma formation. Practical thin films with broadband optical-limiting characteristics can now be fabricated. The optical-limiting threshold achieved here (10 mJ cm^{-2} for a linear transmittance of 70%) for nanosecond pulses in a loose-focus configuration is 5–10 times lower than previously known, which thus sets a new performance benchmark. Our experiments also show that unfunctionalized graphene, which has very limited dispersability, can also exhibit this giant NLO response in an appropriate heavy-atom solvent. This optical-limiting mechanism is therefore a property of the graphene dispersed in the matrix rather than the result of functionalization.

Preparation of functionalized graphene

Solvent-dispersible graphenes were prepared from sub-stoichiometric graphene oxide (sub-GOx) by half-oxidizing graphite and then grafting the sub-GOx with octadecylamine surface chains to give organic-solvent dispersible sheets in the range of 300–500 nm (ref. 17). It is important to distinguish between these sub-GOx[17] and the heavily oxidized GOx that can be obtained by exhaustive oxidation of graphite[18,19], although this distinction is often lost in the literature[20,21]. The fully oxidized stoichiometric GOx does not have π-electrons, but sub-GOx has a significant fraction of sp^2

[1]DSO National Laboratories, 20 Science Park Drive, Science Park I, Singapore 118230, Singapore, [2]Department of Physics, National University of Singapore, Lower Kent Ridge Road, Singapore S117542, Singapore, [3]Department of Chemistry, National University of Singapore, Lower Kent Ridge Road, Singapore S117543, Singapore, [4]Cavendish Laboratory, University of Cambridge, JJ Thomson Avenue, Cambridge CB3 0HE, UK. *e-mail: chmcll@nus.edu.sg; lgeokkie@dso.org.sg

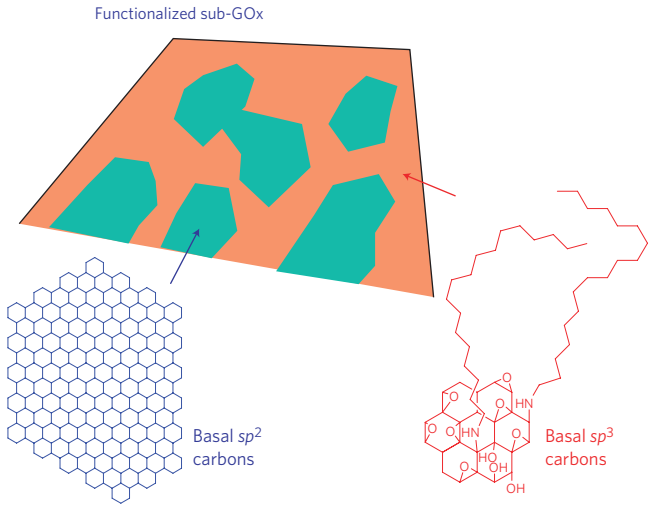

Figure 1 | Schematic structure of a functionalized sub-GOx sheet. The sheet comprises nanographene domains (blue-green) separated by an alkyl-functionalized and oxygenated sp^3 carbon network (orange).

carbon atoms retained in the basal plane which gives it semiconducting and optical properties.

For sub-GOx that is about one-third to half oxidized, the sp^2 carbon atoms are organized into nanographene domains[17], which are quite large 2D π-electron systems with diameters of ~10 nm (estimated by Raman and infrared spectroscopies; Supplementary Section 1), separated by boundaries comprising a network of epoxy and/or hydroxyl-bonded sp^3 carbon atoms (Fig. 1). These domains exhibit broadband electronic absorption that is similar to that of 'perfect' graphene. Furthermore, in contrast to heavily oxidized GOx, sub-GOx can undergo facile thermal re-graphenization by extending the nanographene domains into a 'graphenite' network[22] that shows band-like field-effect transport despite disorder[17]. The sp^3 carbon atoms in the domain boundaries provide sites for chemical functionalization with a variety of alkyl chains and groups[23–25]. These sub-GOx can therefore be regarded as functionalized graphenes that can be dispersible as single sheets in a variety of solvents and film matrices.

The octadecylamine-functionalized sub-GOx nanosheets can be repeatedly isolated in the dry state, and re-dispersed in a variety of organic solvents (up to 15 mg ml^{-1}) and polymer matrices. The alkyl chains prevent the re-stacking of these sheets, and therefore promote their dispersability in various matrices. From here onwards, 'sub-GOx' will refer to this functionalized form. For comparison, we have also prepared and functionalized a heavily oxidized GOx that is closer to the stoichiometric oxide.

Giant optical-limiting effect in graphene–polymer film

Figure 2a shows the UV-vis-NIR transmittance spectrum of a 2.0-μm-thick film of sub-GOx dispersed in bisphenol-A polycarbonate (PC) at a weight ratio of 2.9 w/w%. The film quality is good (inset, Fig. 2a). Differential scanning calorimetry reveals the glass transition temperatures of the polymers in these nanocomposites to be generally upshifted, so the nanosheets are well-dispersed in the film matrices (Supplementary Section 2). The transmittance spectrum of a 2.0-μm-thick film of heavily oxidized GOx in PC at a weight ratio of 4.5 w/w% is also shown for comparison, together with that of sub-GOx dispersed in chlorobenzene (CB, 80 μg ml^{-1}) and ultrasonically exfoliated graphene in 1,2,4-trichlorobenzene (TCB, 30 μg ml^{-1}) in 1.0 mm path length cells.

The absorption of sub-GOx increases towards shorter wavelengths, with a profile that is nearly identical to that of graphene down to the mid-infrared region[17]. The nanographene domains in the sub-GOx therefore have an optical joint density-of-states that is similar to graphene. Curiously, sub-GOx in both chlorobenzene and PC shows an absorption cross-section per basal carbon atom of 2.2×10^{-18} cm^2 at a wavelength of 532 nm, which is also similar to graphene. In contrast, the heavily oxidized GOx has a much lower absorption cross-section (by a factor of two) and shows discernible structures in the short-wavelength region that are characteristic of small π-electron systems.

NLO characteristics were measured using an open-aperture nanosecond *Z*-scan technique (Fig. 2b). The transmittance of the sample was measured as a function of the incident laser fluence, which was varied by translating the sample through the focal plane along its propagation (*Z*) axis. A Q-switched Nd-YAG laser was frequency-doubled to produce 3.5 ns, 532 nm pulses, which were loosely focused by $f/30$ optics to a diameter $2w_o$ of 20 μm ($1/e^2$ intensity) with a Rayleigh length z_R of 600 μm. This Rayleigh length was similar to or much larger than the thickness of the sample (1.0 mm liquid cell, or 2-μm-thick films). Measurements were also made at the fundamental 1,064 nm wavelength.

Figure 2c presents a plot of output fluence F_{out} versus input fluence F_{in} for the sub-GOx/PC film measured in air for 3.5 ns, 1,064 nm pulses. Data were measured over ten spots and averaged. No significant spot-to-spot variation was found. The F_{out}/F_{in} ratio in the limit of zero fluence gives the linear transmittance T of the film. At high fluences, the limiting slope dF_{out}/dF_{in} gives the limiting differential transmittance T'. For this film with $T = 0.85$, the nonlinearity onset fluence F_{on} occurs at 10 mJ cm^{-2}, and the half-transmittance fluence F_{50} (where transmittance falls to 50% of T) occurs at 100 mJ cm^{-2}. Above this, the film exhibits good output clamping characteristics with $T' = 0.17$.

Figure 2d shows the F_{out} versus F_{in} characteristic at a wavelength of 532 nm, and Fig. 2e the corresponding transmittance versus F_{in} characteristic. At this wavelength, the film shows $T = 0.73$, with F_{on} at 10 mJ cm^{-2} and F_{50} at 80 mJ cm^{-2}, and even better output clamping with $T' = 0.055$. These F_{on}, F_{50} and T' values for both wavelengths greatly surpass those of CNT dispersed in poly(methyl methacrylate) (PMMA)[26] measured under similar conditions, by a factor of 5–10. Note that CNT in PMMA is not stable to repeated laser shots, in contrast to these sub-GOx nanocomposites. A more precise comparison will therefore have to be made in liquid dispersions, as presented below. Note also that the PC film does not show any optical limitation, and the heavily oxidized GOx/PC film with the same T gives a considerably weaker optical-limiting effect ($F_{50} =$ 300 mJ cm^{-2} and $T' = 0.25$) (Fig. 2d,e). This shows that the giant NLO response in the sub-GOx/PC film is related to the nanographene domains.

It is clear that the mechanism for this giant optical-limiting effect does not involve the material breakdown that is known to occur at much higher fluences in CBS[3,4], CNT[13,26], and even in graphite[27]. No black spots or pinholes were found by optical microscopy on the films after more than 100 shots at the highest fluences. Moreover, the *Z*-scan characteristic (Fig. 2f) is symmetric before and after traversal through the focus. No irreversible change in the film optical properties occurred due to heating or induced chemical transformation.

Strong solvent/matrix effect on NLO response of graphene

Figure 3a reveals that the NLO characteristics of sub-GOx using 3.5 ns pulses at 532 nm exhibit an unusual and strong dependence on the film matrix. A neat film of the sub-GOx does not in fact give any optical limitation in the measured fluence range. It shows nearly perfect saturable absorption with $T' = 0.97$ above 10 mJ cm^{-2}. The absence of optical limitation in this film is consistent with the behaviour of graphite at similar fluences, over which the photo-excited electron–hole gas relaxes to the *K*-point and recombines

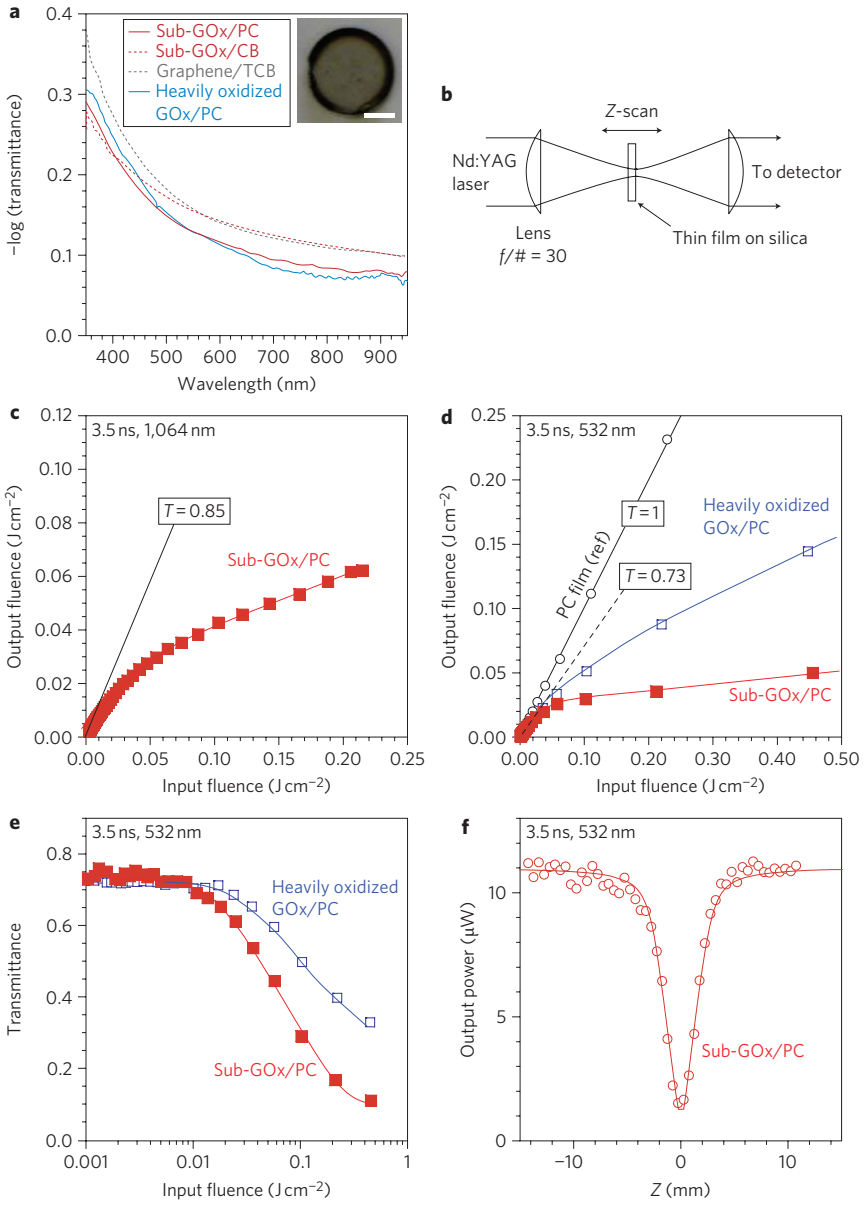

Figure 2 | Linear and nonlinear transmittance characteristics of sub-GOx/PC film. a, UV-vis-NIR spectra of sub-GOx/PC film. The solution spectra are collected in a 1.0 mm path length cell. Spectra of ultrasonically exfoliated graphene dispersed in TCB, sub-GOx in CB and heavily oxidized GOx in PC are also shown for comparsion. Inset: photograph of film cast on fused silica disc (scale bar, 5 mm) showing 70% transmittance over the central region. **b**, Schematic of the *Z*-scan technique. **c**,**d**, Plot of output versus input fluence (red square) for 3.5 ns pulses at 1,064 nm and 532 nm wavelengths, respectively. *T* is the linear transmittance given by the F_{out}/F_{in} ratio in the limit of zero fluence and is 0.85 at 1,064 nm and 0.73 at 532 nm. The PC film is given in **d** as a reference, showing no optical limiting property. **e**,**f**, Plot of transmittance versus input fluence for 3.5 ns pulses at 532 nm and its Z-scan characteristics. The characteristics of heavily oxidized GOx/PC film are also shown in **d** and **e**. All spectra and input fluences are corrected for reflection loss.

over a picosecond timescale, during which the joint density-of-states is blocked and absorption saturates[28,29]. A similar behaviour has also been found in multilayer graphenes[30,31].

The optical-limiting effect emerges when the sub-GOx is dispersed into PMMA, and becomes even stronger in PC. It is therefore clear that the giant optical-limiting effect is not an intrinsic feature of the nanographene domains, but depends on interaction with their environment. To clarify an aspect of this interaction, we conducted the following experiments in liquid cells. These offer a wider range of solvent matrices, and better stability to intense laser pulses due to continuous regeneration of the probe volume.

Figure 3b shows that the sub-GOx can exhibit saturable absorption or reverse saturable absorption depending on the solvent. We have previously established that our sub-GOx disperses as single sheets in these solvents[17]. The sub-GOx in chlorobenzene exhibits strong optical limitation ($F_{on} = 10$ mJ cm^{-2} and $T' = 0.10$) that is comparable to the sub-GOx/PC film, and markedly superior to those of C_{60} (and also phenyl-C_{61}-butyrate methyl ester; data not shown) in toluene and single-walled CNTs in tetrahydrofuran (THF). The wavelength dependence of the optical-limiting response in chlorobenzene was measured using a tunable laser (Supplementary Section 3). The results confirm that this is broadband and extends over the 450–1,064 nm wavelength range, but with a gradual roll off above 700 nm.

This optical limitation effect increases marginally when the solvent is changed to bromobenzene (BB), 1,2-dichlorobenzene

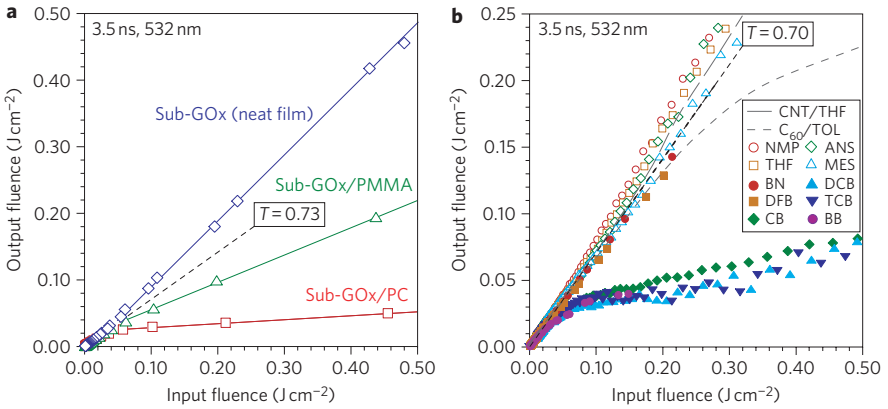

Figure 3 | Strong solvent/matrix effect on the nonlinear optical properties of dispersed sub-GOx. a, Plot of output versus input fluence for a neat film of sub-GOx ($T' = 0.97$), and sub-GOx in PMMA ($T' = 0.40$) and in PC ($T' = 0.055$). T' is the limiting differential transmittance. The linear transmittance T is 0.73 for all films. **b**, Plot of output versus input fluence for sub-GOx dispersed in different solvents compared with C_{60} in TOL and single-walled CNT in THF, all in cells with 1.0 mm path length. NMP, *N*-methylpyrrolidinone; THF, tetrahydrofuran; ANS, anisole; MES, mesitylene; DFB, 1,3-difluorobenzene; BN, benzonitrile; CB, chlorobenzene; BB, bromobenzene; DCB, 1,2-dichlorobenzene; TCB, 1,2,4-trichlorobenzene; TOL, toluene. T is 0.70.

(DCB) or TCB, but diminishes greatly in 1,3-difluorobenzene (DFB) and benzonitrile (BN). It disappears in *N*-methylpyrrolidone (NMP), THF, anisole (ANS) and mesitylene (MES). This last group of solvents in fact causes saturable absorption to emerge ($T' = 0.9$ at $F_{in} = 500$ mJ cm^{-2}), which switches to optical limitation only above 700 mJ cm^{-2}, as previously reported[14–16]. When a small amount of bad solvent was added to the CB cell (for example, 25 vol% ethanol) to cause aggregation of the sub-GOx sheets, the optical limitation disappears. These results show that a strong solvent/matrix effect acts on the dispersed single sheets to cause the NLO response.

The increase in the optical-limiting response across the solvent series DFB << CB < BB, DCB, TCB is characteristic of a marked heavy-atom effect[32]. This effect has been traditionally studied in molecular systems, where the heavy atom promotes intersystem crossing of the excited singlet state to the triplet state by spin–orbit coupling[32]. Its emergence in the nanographene response here is therefore unexpected, and suggests that the excited states have become localized. Charge transfer can be ruled out as the dominant mechanism, because the sub-GOx shows a weaker optical-limiting effect in BN (and DFB) than in bromobenzene, which is the less electronegative solvent. The possibility that the solvent perturbs the ground state of the nanographene domains in different ways has also been ruled out. Raman spectroscopy shows no difference in the *D* and *G* bands of the sub-GOx in different solvents (Supplementary Section 4). Incidentally, the solvent microbubble mechanism can also be ruled out by lack of dependence on the solvent boiling point (cf. TCB, DCB and CB).

Figure 4 shows that ultrasonically exfoliated graphene sheets in TCB give similar optical-limiting characteristics as sub-GOx in chlorobenzene, but the heavily oxidized GOx is decidedly inferior. It has been shown previously that these graphenes do not show optical-limiting effects in NMP and DMF over this fluence range[14–16].

It is therefore clear that one aspect of the unusual optical-limiting behaviour of dispersed graphene sheets relates to the formation of localized and highly absorbing triplet-like states. In the following, we will use nanosecond pump–probe spectroscopy to measure the transient response of dispersed sub-GOx across the F_{on} threshold to reveal further evidence of localized excited states.

Transient absorption spectroscopy

The probe pulses were prepared by broadband non-collinear parametric amplification seeded by a 1 kHz, 800 nm, 90 fs output of a Ti:sapphire (Solstice) regenerative amplifier. The pump pulses (532 nm, 0.5 ns) were the frequency-doubled output of a Q-switched Nd:YVO_4 laser, triggered electronically by the Solstice through a delay generator. The temporal resolution was better than 0.7 ns. The pump and probe beams polarized at the magic angle were both focused onto the cell in a near-collinear geometry. A split-off reference was also incident a small distance away to normalize for pulse variations. The transmitted probe and split-off reference were dispersed by a grating onto two parallel silicon diode arrays. The differential transmittance was obtained by comparing the probe normalized by the split-off reference, with and without the pump in adjacent pulses, and then presented as $\Delta T/T$, defined as $(T_{on} - T_{off})/T_{off}$ in real time, where T_{on} and T_{off} are, respectively, the transmittance with and without the pump pulses. The average pump fluence reported here is weighted by the probe intensity profile, and therefore differs from the definition

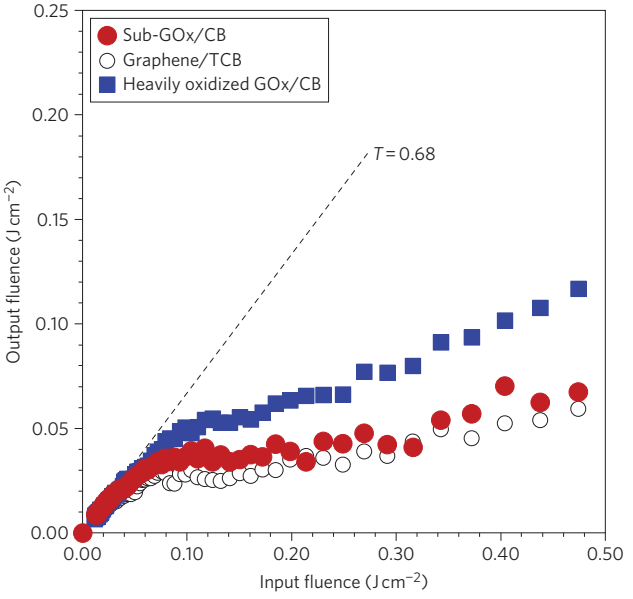

Figure 4 | Nonlinear transmittance characteristics of ultrasonically exfoliated graphene, sub-GOx and heavily oxidized GOx. Plot of output versus input fluence for ultrasonically exfoliated graphene in TCB, sub-GOx in CB and heavily oxidized GOx in CB. Linear transmittance T is 0.68. Data are for 3.5 ns pulses at 532 nm collected in a 1.0 mm path length cell.

of fluence in the *Z*-scan. This was varied between 2 and 90 mJ cm^{-2} by varying the incident power and focusing optics.

Figure 5a–d show the $\Delta T/T$ spectra of sub-GOx in chlorobenzene for different probe delays and pump fluences. Zero delay corresponds to coincidence of the centres of the pump and probe pulses. For a pump fluence of 2 mJ cm^{-2}, which is well below the nonlinearity onset, the transient response is a spectrally flat photo-induced bleaching (that is, positive $\Delta T/T$). This is characteristic of blocking of the optical joint density-of-states by the photo-excited electron–hole plasma, which indicates that the electrons and holes are substantially delocalized within the nanographene domains. There is an unusually long tail with a lifetime of ~20 ns, which suggests trapping. Similar results have been obtained in other solvents including mesitylene and anisole.

At a higher fluence of 20 mJ cm^{-2}, the photo-bleaching is still present, but is attenuated by induced absorptions that emerge within the first 0.2 ns (instrument-limited), with dips at 2.1, 1.9 and 1.75 eV. At 30 mJ cm^{-2}, the photo-absorption dips become more pronounced and dominate the response after ~2 ns. At 90 mJ cm^{-2}, the transient response is firmly photo-induced absorption across the entire spectral window, beginning at the sub-nanosecond timescale. There is a roll-off of the absorption beyond 700 nm, as found also in the wavelength-dependent optical-limiting data. Absorption bands are again found at 2.15, 1.95 and 1.80 eV. The dynamics is complicated by the presence of slow-rise components with rise times of 1–3 ns, and multiple decay lifetimes from 6 to 45 ns.

The fast emergence of transient absorption demonstrates that the leading mechanism for the giant optical limitation effect in liquid cells is excited-state absorption. This absorption is characteristic of localized excited states typically associated with molecular π-electron systems. The average band spacing is 0.15–0.20 eV, which coincides with the Raman modes of graphene (*G* band, 0.195 eV; *D* band, 0.165 eV), and so we assign to the vibronic spacing of excitonic states. This interpretation receives support from (i) the heavy-atom effect, (ii) the large apparent optical cross-section of these states, which we estimate from the T'/T ratio to be at least ~1×10^{-17} cm^2 per basal carbon at 532 nm wavelength, and (iii) long excitation lifetimes.

The fluence- and time-dependent crossover from induced transparency to induced absorption is different from the usual behaviour of small π-electron systems[32]. These characteristics suggest that the long-lived excitons here are generated not by direct excitation or the usual singlet → triplet intersystem crossing, but by interactions within the initial electron–hole gas in a nonlinear mechanism. This leads us to speculate that the initial electron–hole gas condenses to triplet-like excitons when promoted by spin–orbit coupling with heavy atoms, as schematically illustrated by path (i) of Fig. 6a. In contrast, in graphite or multilayer graphenes in which the inner layers are effectively isolated from the environment, the electron–hole gas cools and recombines rapidly (Fig. 6b). The mechanism in solid films is even less well understood, but must nevertheless also derive from localization effects. The apparent dependence on the electron-accepting ability of the matrix, however, hints at a photo-induced charge-transfer mechanism (path (ii) of Fig. 6a). This possibility is suggested by the significant increase in absorption of sub-GOx over when *p*-doped with a powerful electron–acceptor tetrafluorotetracyanoquinonedimethane (Supplementary Section 5). The apparent absorption cross-section of the doped holes (3×10^{-17} cm^2 per carbon atom) is one order of magnitude larger than the ground-state absorption of graphene, and extends over a wide vis–NIR region. This can explain the excellent output clamping obtained. This large oscillator strength is characteristic of localization and reminiscent of a polaronic character well known in π-conjugated polymers[33–35]. This mechanism appears to be remarkably efficient in the solid film and shows little roll-off in efficiency, even to a wavelength of 1,064 nm.

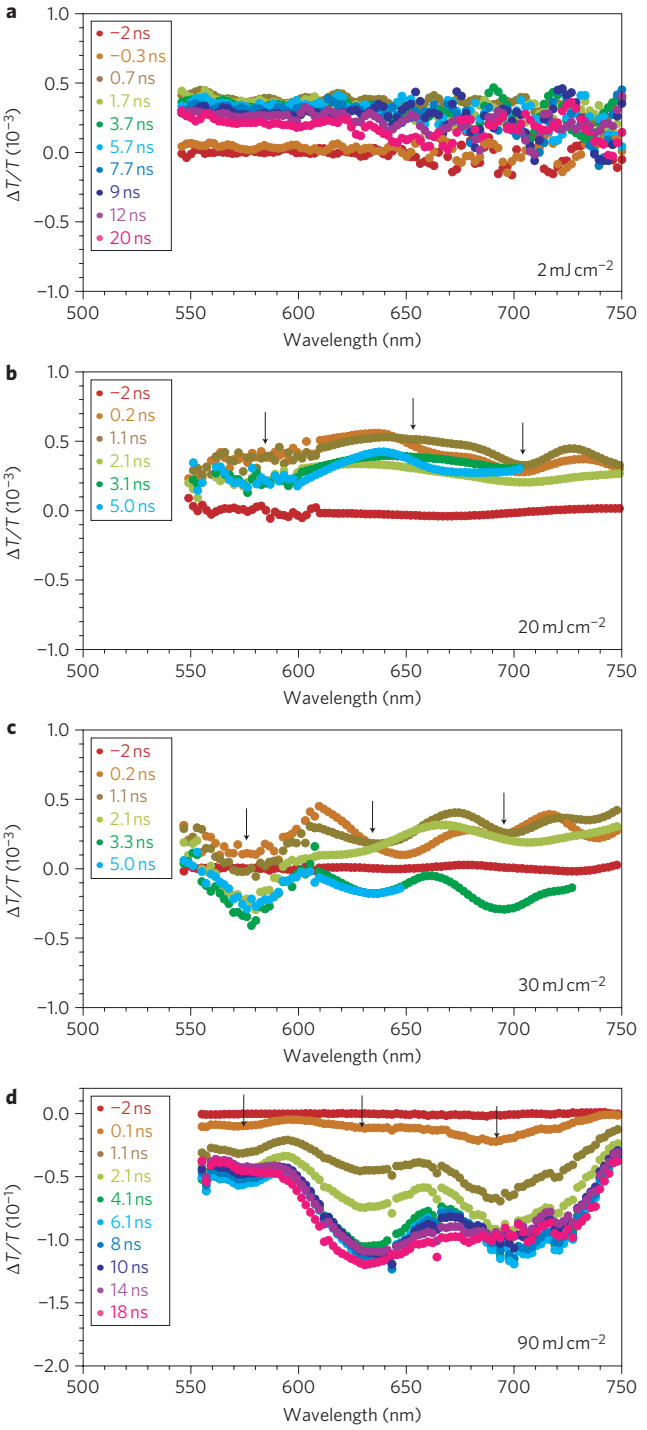

Figure 5 | Normalized transient transmittance $\Delta T/T$ spectra as a function of pump–probe delay for sub-GOx dispersed in chlorobenzene at a pump wavelength of 532 nm. a–d, Pump fluence: 2 (**a**), 20 (**b**), 30 (**c**) and 90 mJ cm^{-2} (**d**). This pump fluence is weighted by the probe intensity profile. The temporal resolution is 0.7 ns due to pump width and jitter. Repetition rate, 500 Hz. The 525–550 nm region is masked off by a notch filter. For **b** and **c**, the 610–750 nm region has been smoothed to reduce clutter.

In summary, we have found an unusually efficient nonlinear optical-limiting behaviour that occurs in graphene and alkyl-functionalized sub-GOx when they are dispersed as single sheets in appropriate solvents or film matrices. As a result, practical broadband optical limiters in both liquid cells and thin films or coatings

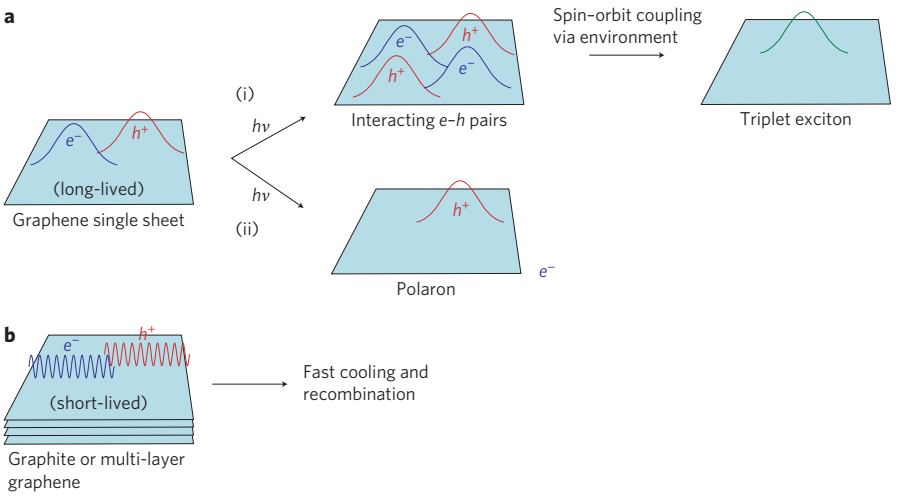

Figure 6 | Schematic outlining new optical-induced absorption mechanisms. a, Photoexcitation of a dispersed graphene single sheet gives long-lived electron–hole pairs. Further excitation causes the appearance of localized states such as (i) excitons (neutral excited state) or (ii) polarons (charged excited state) due to interactions. **b**, For comparison, graphite gives on electron–hole gas that is very short-lived due to fast cooling and recombination.

can now be constructed with performances exceeding those of other carbon nanostructures by a factor of 5–10. We have outlined a new phenomenon in which the initially delocalized electron–hole gas localizes at high excitation densities in the presence of heavy atoms, to give strongly absorbing excitons. The resultant excited-state absorption mechanism can therefore be very effective. In essence, the broadband absorption advantage of large π-electron systems has been combined with the intense excited-state absorption advantage of small π-electron systems.

Methods

Materials. Sub-GOx was prepared by oxidation of synthetic graphite (496596, Sigma Aldrich) using a modified Staudemaier oxidation[17]. The graphite was reacted with a mixture of concentrated sulphuric acid, fuming nitric acid and potassium chlorate at 0–5 °C (1 h), held at room temperature for seven days, then washed extensively with Millipore water to give a product with an empirical formula of $C_{2.0}O_{0.77}$ (according to combustion analysis). This was functionalized by mixing sub-GOx (10 mg) with octadecylamine (ODA, 100 mg) and 1,3-diisopropylcarbodiimide (60 μl) in DCB (5 ml) and heating with intermittent ultrasonication to 80 °C (24 h) under a nitrogen blanket to give a homogeneous black dispersion. This dispersion (1 ml) was mixed with THF (5 ml), briefly ultrasonicated, then centrifuged (8,000 r.p.m., 5,580*g*) for 1 h to separate the sediment from the supernatant, which contains the functionalized sub-GOx. The functionalized sub-GOx was then purified by precipitation with ethanol (5 ml), centrifugation (1,000*g*, 1 h), and re-dispersion in THF (0.25 ml), repeated three times, and dried under vacuum at room temperature. This purified material had an empirical formula $C_{2.0}O_{0.77}$–$ODA_{0.085}$, with an average sheet size of 500 nm (ref. 17). The fraction of sp^2 carbon atoms ($f\pi$) in the basal plane was evaluated to be ~50–60% by X-ray photoemission spectroscopy. The nanographene domains in these functionalized sheets were estimated to be ~6–18 nm across (Supplementary Section 1). Heavily oxidized GOx was also prepared as above, but with potassium dichromate as the oxidant, to give an empirical formula of $C_{2.0}O_{1.73}$ with $f\pi \approx 0.25$. This material was also functionalized in the same way.

Liquid-cell samples. Synthetic graphite (496596, Sigma Aldrich) was dispersed in 1,2,4-trichlorobenzene (TCB) by ultrasonication (1 mg in 1 ml, 2 h), then centrifuged at 1,000*g* to leave a supernatant containing ~30 μg ml^{-1} of dispersed graphene sheets. Functionalized sub-GOx was dispersed in various solvents, including chlorobenzene, with brief ultrasonication. To achieve an internal transmittance of 0.7 at a wavelength of 532 nm, through a 1.0 mm path length, we typically require 80 μg ml^{-1}.

Thin-film samples. To obtain functionalized sub-GOx dispersed in PC, a solution of PC (400 mg ml^{-1} in 10:1 v/v chlorobenzene:TCB) was first prepared at 120 °C in the nitrogen glovebox. Functionalized sub-GOx (6.0 mg) was separately dispersed in chlorobenzene (0.50 ml) and added to the PC solution (0.50 ml) with ultrasonication to aid complete dispersion, giving 2.9 w/w% functionalized sub-GOx to total solids. A 2.0-μm-thick film was formed by spin-casting at 3,000 r.p.m. on a fused silica disc (diameter, 13 mm), then baked at 90 °C (hotplate, 5 min) to dry off the solvent.

For functionalized heavily oxidized GOx dispersed in PC, functionalized heavily oxidized GOx (9.3 mg) was first dispersed in chlorobenzene (0.50 ml). To this was added the PC solution (0.5 ml) with ultrasonication to give 4.5 w/w% heavily oxidized GOx to total solids. A 2.0-μm-thick film was formed by spin-casting as above.

For functionalized sub-GOx dispersed in PMMA, a solution of PMMA (400 mg ml^{-1} in chlorobenzene) was prepared at 65 °C. Functionalized sub-GOx (12 mg) was added to this solution (1.0 ml) with ultrasonication to give 2.9 w/w% sub-GOx to total solids. A 3.0-μm-thick film was formed by spin-casting at 1,000 r.p.m. For neat sub-GOx film, functionalized sub-GOx dispersed in THF (0.3 mg ml^{-1}) was drop-cast.

Received 16 November 2010; accepted 7 July 2011;
published online 21 August 2011

References

1. Tutt, L. W. & Boggess, T. F. A review of optical limiting mechanisms and devices using organics, fullerences, semiconductors and other materials. *Prog. Quantum Electron.* **17,** 299–338 (1993).
2. Sun, Y. P. & Riggs, J. E. Organic and inorganic optical limiting materials: from fullerenes to nanoparticles. *Int. Rev. Phys. Chem.* **18,** 43–90 (1999).
3. Mansour, K., Soileau, M. J. & Van Stryland, E. W. Nonlinear optical properties of carbon-black suspensions (ink). *J. Opt. Soc. Am. B* **9,** 1100–1109 (1992).
4. Nashold, K. M. & Walter, D. P. Investigations of optical limiting mechanisms in carbon particle suspensions and fullerene solutions. *J. Opt. Soc. Am. B* **12,** 1228–1237 (1995).
5. Chen, P. *et al.* Electronic structure and optical limiting behavior of carbon nanotubes. *Phys. Rev. Lett.* **82,** 2548–2551 (1999).
6. Vivien, L. *et al.* Single-wall carbon nanotubes for optical limiting. *Chem. Phys. Lett.* **307,** 317–319 (1999).
7. Riggs, J. E., Walker, D. B., Carroll, D. L. & Sun, Y. P. Optical limiting properties of suspended and solubilized carbon nanotubes. *J. Phys. Chem. B* **104,** 7071–7076 (2000).
8. Brandelik, D. *et al.* Nonlinear optical properties of buckminsterfullerene solutions. *Mater. Res. Soc. Symp. Proc.* **247,** 361–366 (1992).
9. Tutt, L. W. & Kost, A. Optical limiting performance of C_{60} and C_{70} solutions. *Nature* **356,** 225–226 (1992).
10. Perry, J. W. *et al.* Organic optical limiter with a strong nonlinear absorptive response. *Science* **273,** 1533–1536 (1996).
11. de la Torre, G., Vázquez, P., Agulló-López, F. & Torres, T. Role of structural factors in the nonlinear optical properties of phthalocyanines and related compounds. *Chem. Rev.* **104,** 3723–3750 (2004).
12. Senge, M. O. *et al.* Nonlinear optical properties of porphyrins. *Adv. Mater.* **19,** 2737–2774 (2007).
13. Vivien, L. *et al.* Picosecond and nanosecond polychromatic pump–probe studies of bubble growth in carbon-nanotube suspensions. *J. Opt. Soc. Am. B* **19,** 208–214 (2002).
14. Wang, J. *et al.* Broadband nonlinear optical response of graphene dispersions. *Adv. Mater.* **21,** 2430–2435 (2009).
15. Zhao, B. *et al.* Nonlinear optical transmission of nanographene and its composites. *J. Phys. Chem. C* **114,** 12517–12523 (2010).
16. Feng, M., Zhan, H. & Chen, Y. Nonlinear optical and optical limiting properties of graphene families. *Appl. Phys. Lett.* **96,** 033107 (2010).

17. Wang, S. *et al.* Band-like transport in surface-functionalised highly solution-processable graphene nanosheets. *Adv. Mater.* **20,** 3440–3446 (2008).
18. Lerf, A., He, H., Forster, M. & Klinowski, J. Structure of graphite oxide revisited. *J. Phys. Chem. B* **102,** 4477–4482 (1998).
19. Szabó, T. *et al.* Evolution of surface functional groups in a series of progressively oxidized graphite oxides. *Chem. Mater.* **18,** 2740–2749 (2006).
20. Cai, W. W. *et al.* Synthesis and solid-state NMR structural characterization of C13-labeled graphite oxide. *Science* **321,** 1815–1817 (2008).
21. Gao, W., Alemany, L. B., Ci, L. & Ajayan, P. M. New insights into the structure and reduction of graphite oxide. *Nature Chem.* **1,** 403–408 (2009).
22. Chua, L.-L. *et al.* Deoxidation of graphene oxide nanosheets to extended graphenites by 'unzipping' elimination. *J. Chem. Phys.* **129,** 114702 (2008).
23. Stankovich, S. *et al.* Graphene-based composite materials. *Nature* **442,** 282–286 (2006).
24. Schniepp, H. C. *et al.* Functionalised single graphene sheets derived from splitting graphite oxide. *J. Phys. Chem. B* **110,** 8535–8539 (2006).
25. Eda, G. & Chhowalla, M. Chemically derived graphene oxide: towards large-area thin-film electronics and optoelectronics. *Adv. Mater.* **22,** 2392–2415 (2010).
26. Sun, X. *et al.* Broadband optical limiting with multiwalled carbon nanotubes. *Appl. Phys. Lett.* **73,** 3632–3634 (1998).
27. Reitze, D. H., Wang, X., Ahn, H. & Downer, M. C. Femtosecond laser melting of graphite. *Phys. Rev. B* **40,** 11986–11989 (1989).
28. Seibert, K. *et al.* Femtosecond carrier dynamics in graphite. *Phys. Rev. B* **42,** 2842–2851 (1990).
29. Breusing, M., Ropers, C. & Elsaesser, T. Ultrafast carrier dynamics in graphite. *Phys. Rev. Lett.* **102,** 086809 (2009).
30. Bao, Q. *et al.* Atomic-layer graphene as a saturable absorber for ultrafast pulsed lasers. *Adv. Funct. Mater.* **19,** 3077–3083 (2009).
31. Kumar, S. *et al.* Femtosecond carrier dynamics and saturable absorption in graphene suspensions. *Appl. Phys. Lett.* **95,** 191911 (2009).
32. Turro, N. J. *Modern Molecular Photochemistry* (University Science Books, 1991).
33. Zhuo, J. M. *et al.* Direct evidence for delocalisation of charge carriers at the Fermi level in a doped conducting polymer. *Phys. Rev. Lett.* **100,** 186601 (2008).
34. Zhou, M. *et al.* The role of delta-doped interfaces for ohmic contacts to organic semiconductors. *Phys. Rev. Lett.* **103,** 036601 (2009).
35. Clark, J., Silva, C., Friend, R. H. & Spano, F. C. Role of intermolecular coupling in the photophysics of disordered organic semiconductors: aggregate emission in regioregular polythiophene. *Phys. Rev. Lett.* **98,** 206406 (2007).

Acknowledgements

L.L.C. acknowledges the Ministry of Education Academic Research Fund for funding. P.K.H.H. acknowledges the Defence Science and Technology Agency for Temasek Young Investigator's award. R.H.F. acknowledges the Tan Chin Tuan Foundation for National University of Singapore Centennial Professorship. J.C. acknowledges the Royal Society for a Dorothy Hodgkin fellowship.

Author contributions

G.K.L. and L.L.C conceived the idea, performed the experiment and analysed the data. J.C. performed the experiments and analysed the data. R.H.F and P.K.H.H. analysed the data. Z.L.C. and R.G.S.G. synthesized and characterized the graphene materials. W.H.N and H.W.T. contributed to *Z*-scan measurement setup. G.K.L, J.C., R.H.F., P.K.H.H. and L.L.C. contributed to writing the paper.

Additional information

The authors declare no competing financial interests. Supplementary information accompanies this paper at www.nature.com/naturephotonics. Reprints and permission information is available online at http://www.nature.com/reprints. Correspondence and requests for materials should be addressed to G.K.L. and L.L.C.